ISSN 1063-7729, Astronomy Reports, 2006, Vol. 50, No. 1, pp. 68–78. © Pleiades Publishing, Inc., 2006.
Original Russian Text © I.M. Chertok, 2006, published in Astronomicheskiĭ Zhurnal, 2006, Vol. 83, No. 1, pp. 76–87.

Large-Scale Activity in Major Solar Eruptive Events of November 2004 According to SOHO Data

I. M. Chertok

Pushkov Institute of Terrestrial Magnetism, Ionosphere, and Radio Wave Propagation, Russian Academy of Sciences, Troitsk, Moscow oblast, 142190 Russia

Received June 10, 2005; in final form, July 6, 2005

Abstract—Data obtained with the EIT UV telescope and LASCO coronagraph of the SOHO satellite are used to analyze large-scale solar disturbances associated with a series of major flares and coronal mass ejections that occurred in the late decline phase of cycle 23, on November 3–10, 2004, and gave rise to strong geomagnetic storms. Derotated fixed-base difference heliograms taken in the 195 Å coronal channel at 12-min intervals and in the various-temperature 171, 195, 284, and 304 Å channels at 6-h intervals indicate that these disturbances were global and homologous; i.e., they had similar characteristics and affected the same structures. Almost all of the nine events of this series included two recurrent systems of large-scale dimmings (regions of reduced intensity with lifetimes of 10–15 h): (a) transequatorial dimmings connecting a northern near-equatorial eruption center with a southern active region and (b) northern dimmings covering a large sector between two coronal holes. In this northern sector, coronal waves (brightenings propagated from the eruption center at speeds of several hundred km/s) were observed ahead of the expanding dimmings. The brightest, central part of the halo-type coronal mass ejection in each event corresponded to the northern dimming system. The properties of the dimmings and coronal waves and the relationship between them are discussed on the basis of the results obtained. We find that the eruption of large coronal mass ejections involves structures of the global solar magnetosphere with spatial scales far exceeding the sizes of active regions and normal activity complexes.

PACS numbers : 96.60.P
DOI: 10.1134/S1063772906010082

1. INTRODUCTION

A number of violent outbursts of activity were characteristic of the decline phase of the 23rd 11-year solar cycle. These included series of major flares and large coronal mass ejections (CMEs), accompanied by considerable interplanetary and geophysical disturbances, in particular, extremely strong geomagnetic storms and intense fluxes of energetic particles. Such activity outbursts occurred in October and November 2003, November 2004, and January 2005.

Many studies have been dedicated to various aspects of the extremely high, unparalleled activity in October and November 2003, which was recorded during two transits of a complex of three large active regions across the solar disk (see, e.g., [1, 2]). The solar manifestations of this activity on scales comparable to the radius, or even the diameter, of the visible disk were analyzed in [3, 4] based on data from the SOHO/EIT [5] and CORONAS F/SPIRIT [6] EUV telescopes. In particular, such CME-related large-scale phenomena as dimmings and coronal waves were considered. Recall that dimmings, or transient coronal holes [7–13], are regions of reduced soft-X-ray and EUV intensity with lifetimes of several hours to a day, which form after a CME event in the neighborhood of an eruption center (for example, at the periphery of a pre-eruption sigmoidal structure), and can, in addition, cover a considerable portion of the solar disk. Dimmings trace the structures involved in the CME process, and are commonly interpreted as the result of a complete or partial opening (stretching) of the coronal magnetic fields inside these structures in the course of a CME event that results in evacuation of the matter and corresponding reduction of the emission intensity. A coronal wave is a brightening that propagates from an eruption center at a speed of several hundred km/s, and can be observed either ahead of or independently of developing dimmings [3, 4, 13–18]. Such a wave is regarded as either an MHD disturbance—a coronal analog of chromospheric Moreton waves observed in Hα [19]—or the result of plasma compression at the propagating boundary of dimmings, i.e., regions of open magnetic-field lines [20–22].

In this paper, we analyze CMEs, large-scale

dimmings, and coronal waves in a series of eruptive events that occurred in November 2004, using data from the SOHO/LASCO white-light coronagraph [23] and the SOHO/EIT UV telescope. In addition to considering the characteristics of large-scale manifestations of CMEs in this series of active events, we aim to acquire new information on the properties of dimmings and coronal waves, the relationship between them, the homology of such disturbances in recurrent events, etc. Section 2 describes the general properties of the activity and the technique we employed to analyze the EIT and LASCO-coronagraph data. Some characteristics of the most important CMEs are considered in Section 3. An analysis of the four most violent and representative events with large-scale (global) homologous disturbances on the disk is given in Section 4. The results obtained, including the properties of the dimmings and coronal waves, are discussed in Section 5, which also compares this activity outburst with other series of major eruptive events.

2. CHARACTERIZATION OF ACTIVITY AND THE ANALYSIS TECHNIQUE

The solar-activity outburst considered here and the accompanying space-weather disturbances in November 2004 (see [24] for a review) were related to the rapid growth of region 696 on the disk (with Carrington coordinates of N09, L = 026; Fig. 1). According to the data presented in the *Preliminary Report and Forecast of Solar Geophysical Data* (http://www.sel.noaa.gov/weekly/pdf/prf1523.pdf and 1524.pdf), from November 1 (a heliographic latitude of E63) to November 6 (W08), the sunspot area in this region grew from 60 to 910 millionths of the hemisphere, the number of spots increased from 6 to 33, and the magnetic configuration evolved from a simple (β) to a complex, flare-producing ($\beta\gamma\delta$) configuration. After November 6, the number and area of spots started decreasing, with new increases on November 8 (to 48 in number) and November 9 (to 730 millionths of the hemisphere in spot area). As we will see below, region 695 (S14, L = 045), located somewhat to the west of region 696 and to the south of the solar equator, and possibly also the southwestern region 693 (S14, L = 076), were involved in the CME and dimming-formation process. Coronal holes (CHs) also played an important role, especially those that occupied a large area in the northern hemisphere (CH3, CH4) and the narrow transequatorial coronal hole CH2, which was located west of the structure connecting regions 696 and 695 (Fig. 1).

The violent evolution of region 696 was accompanied by a high flare activity. During the transit of the region across the disk, 13 flares of X-ray class M and two flares of class X occurred. This high flare activity was accompanied by very significant eruptive activity. Many major CMEs were recorded by the SOHO/LASCO coronagraph from November 3 to 10, including nine halo-type CMEs that glowed over a considerable portion of the occulting disk of the coronagraph or of the entire disk.

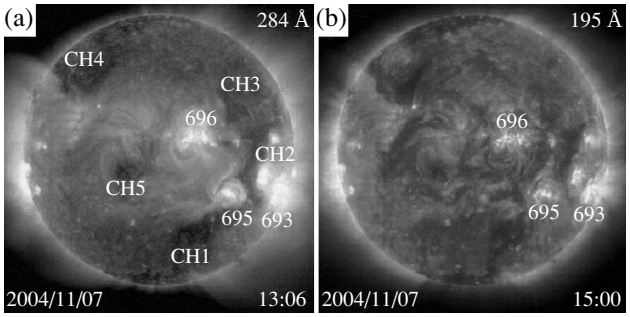

Fig. 1. SOHO/EIT heliograms taken in the (a) 195 Å and (b) 284 Å EUV channels, which illustrate the situation on the solar disk (the locations of active regions and coronal holes (CH)) on November 7, 2004.

Following [3, 11, 12, 25], in our analyses of dimmings and coronal waves in the EUV range by the EIT data, we use the method of derotated, fixed-base difference images formed in two steps. First, to perform the derotation (compensation for the rotation of the Sun), the projection of the solar spherical surface onto the sky plane is rotated within the disk in three dimensions, so as to reduce all frames to the same time. Next, the same background image obtained before the event is subtracted from all subsequent heliograms. This makes it possible to use the EIT data to investigate the development of dimmings over many hours—not only from the images obtained in the 195 Å channel at 12-min intervals, but also from the heliograms taken in the 171 and 284 Å coronal channels, as well as in the 304 Å transition-region channel, at intervals of 6 h. Recall that the 171, 195, and 284 Å coronal channels are sensitive to plasma at temperatures of 1.2, 1.5, and 2.0 MK, while the 304 Å channel contains a transition-region HeII line (0.08 MK) and a less intense coronal SiXI component (1.6 MK) [5].

The fixed-base difference derotated images differ substantially from the widely used running difference images. The latter are formed by subtracting each frame from the next. In essence, such images represent the derivative of the brightness variations, and therefore do not reveal a real spatial structure of disturbances; they are, however, useful, e.g., for identifying coronal-wave fronts.

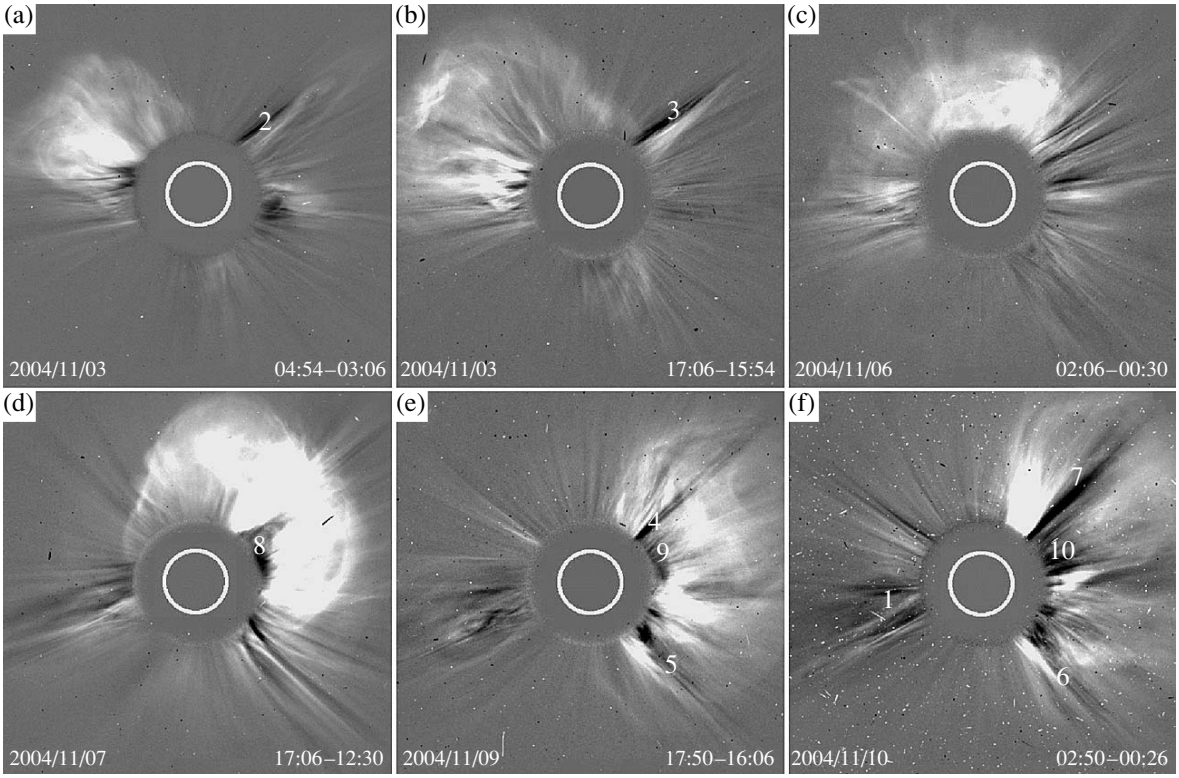

Fig. 2. Fixed-difference images of CMEs during six eruptive events in November 2004 obtained by the SOHO/LASCO/C2 white-light coronagraph. The date of each event and the corresponding times (UT) of the considered and subtracted images are given at the bottom of the images.

We also used fixed-base difference images in our study (but without derotation) to display CMEs at heliocentric distances from 2.5 to 32 $R_\odot$, based on data from the two LASCO coronagraphs. These images trace the development of CMEs in the sky plane via comparison with a background, pre-eruption coronal image. The original FITS files were taken from the EIT catalog (http://umbra.nascom.nasa.gov/eit/eit-catalog.html) and LASCO catalog (http://lasco-www.nrl.navy.mil/cgi-bin/lwdb/lasco/images/form). In view of space limitations, we present below only the most necessary illustrations. Various additional materials concerning the events studied are available via http://helios.izmiran.troitsk.ru/lars/Chertok/04_11/index.html in the form of images and computer movies.

3. CORONAL MASS EJECTIONS

Figure 2 shows fixed-base difference images of six of the nine halo CMEs recorded by the LASCO/C2 coronagraph from November 3–10, 2004. The appearance of these CMEs in the sky plane suggests that they have a large-scale, or even global, character. The linear sizes of the CMEs are much larger than the diameter of the visible solar disk, even at heliocentric distances as short as several $R_\odot$, and the brightest loop structures of the CMEs cover a wide range of position angles, from several tens of degrees to almost 180°. The location of the most significant dimmings (see below) was such that, during the transit of region 696 across the disk, these bright CME features passed from the northeastern to the northern, and then to the northwestern sector of circumsolar space. The glow that was observed near other sectors of the limb testifies to the large angular sizes of the CMEs and the possible presence of a significant velocity component normal to the sky plane—in this case, toward the Earth.

According to the data of the LASCO/C2 and C3 coronagraphs (http://cdaw.gsfc.nasa.gov/CME_list/), three CMEs were observed on November 3–6 (Figs. 2a–2c), when the main eruption source (region 696) was on the eastern half of the disk. They had moderate speeds in the sky plane, from 650 to 1050 km/s. The highest speeds, from 1760 to >2500 km/s, were noted for three CMEs (Figs. 2d–2f) that occurred on November 7, 9, and 10, during the approach of the eruption source to the western limb.

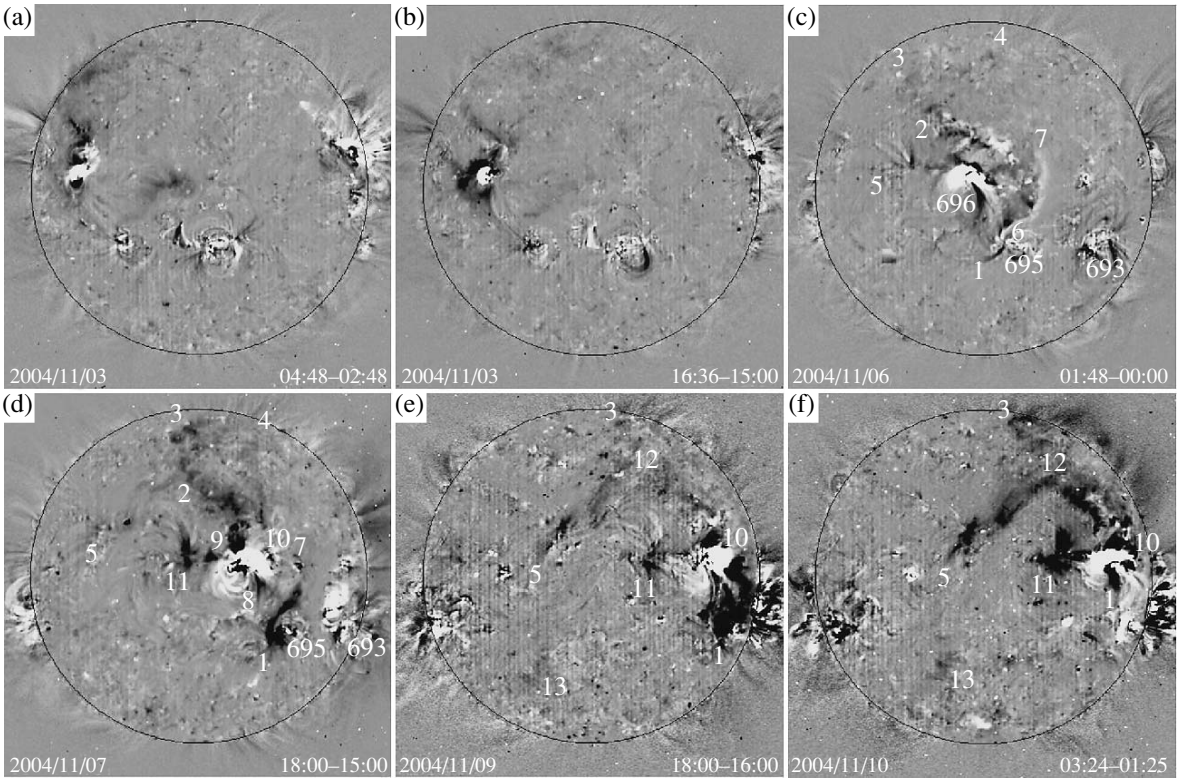

Fig. 3. Derotated fixed-difference SOHO/EIT images taken in the 195 Å channel and showing large-scale disturbances—in particular, dimmings (dark structures)—in six eruptive events of November 2004. The time is indicated as in Fig. 2.

The specific properties of the fixed-difference images enable us to identify changes in the structure of the corona that occurred during an event due to a CME eruption or for other reasons. In particular, dark features in such images correspond to structures that appeared bright before the event, but became fainter in the course of their evolution and changed their location or erupted in association with a CME. In particular, the dark feature 1 over the southeastern limb in the event of November 10 (Fig. 2f) marks the location where a relatively narrow CME was observed two hours earlier, without any relation to the considered activity. On the other hand, some quasi-radial dark features siding with similar bright structures suggest the occurrence of a considerable CME-induced displacement of coronal rays in these cases. In particular, such displacements are visible in two events of November 3 (Figs. 2a, 2b) over the northwestern limb (features 2, 3), the event of November 9 (Fig. 2e) over the northwestern and the southwestern limb (features 4, 5), the event of November 10 (Fig. 2f) over the southwestern (feature 6) and, possibly, the northwestern limb (feature 7).

The corresponding original LASCO movies (see the web site mentioned at the end of Section 2) demonstrate that not only displacements, but also oscillations of the coronal rays relative to their pre-event positions occur fairly often. An analysis of such cases shows that after the first deflection of the coronal ray in the direction of the CME expansion, the ray exhibits an opposite displacement, crosses its initial location, changes its direction of movement again, and gradually returns to a location close to the initial one. The amplitude of these oscillations (the range of position angles) is comparable to the angular width of the coronal ray, and their characteristic times are tens of minutes. The oscillatory process starts at small heliocentric distances and gradually spreads to larger heights in a wavelike manner. The vertical extent of the wave is of the order of several $R_\odot$. It is characteristic that such disturbances involve coronal rays located at considerable distances from the central axis of the CME. This presents additional evidence for the fact that large CMEs produce strong disturbances over a very extensive region of the corona.

The coronal rays encompassed by the main (brightest) part of the CME may likely be ejected as part of the CME. This is the case, e.g., for the dark and extended in position angle regions 8, 9, and 10 in the events of November 7 (Fig. 2d), 9 (Fig. 2e), and 10 (Fig. 2f), respectively.

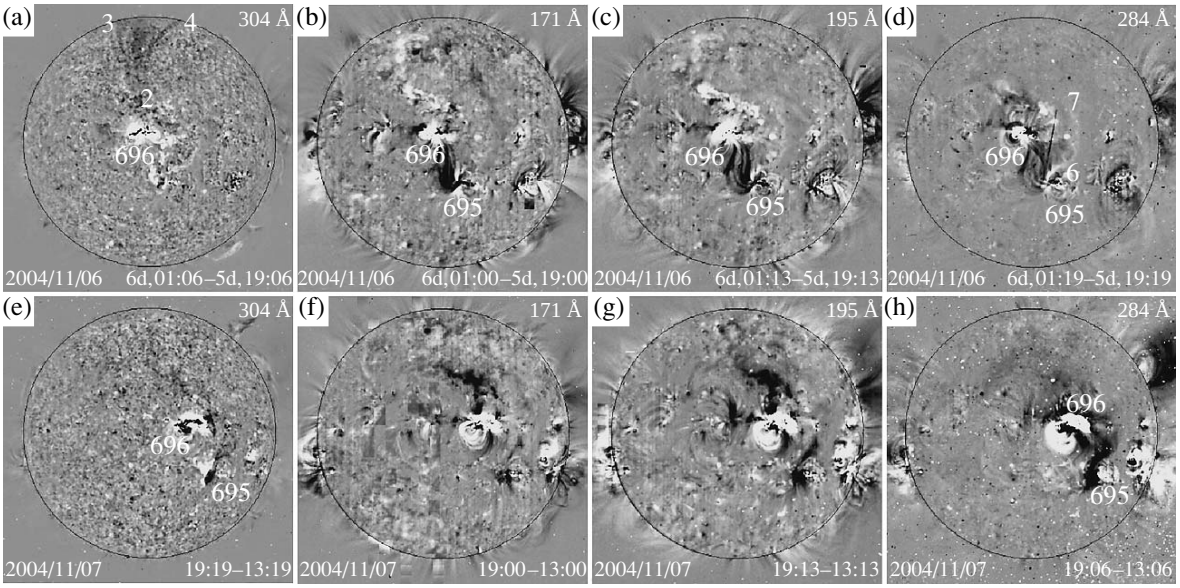

Fig. 4. Derotated fixed-difference SOHO/EIT heliograms taken at a 6-h interval in the 304, 171, 195, and 204 Å channels, illustrating dimmings in channels corresponding to different temperatures for the eruptive events of November 6 and 7, 2004. The time is indicated as in Fig. 2.

4. DIMMINGS AND CORONAL WAVES

In this section, we consider the eruptive events of November 6 and 7, which were associated with large-scale dimmings and coronal waves and produced strong geomagnetic storms with $D_{st} = -373$ and -289 nT, and the events of November 9 and 10, which involved even larger-scale (global), homologous disturbances on the disk, as events typical of the activity outburst of November 2004.

4.1. Event of November 6, 2004

This event included a long-duration, three-component flare of class 2N/M9.3 in the central region of the disk (coordinates N09 E05) with its maximum at 00:34 UT and a halo CME with the brightest features over the northern limb and a distinct glow expanding in both directions around the remainder of the occulting disk of the coronagraph (Fig. 2c). The difference EIT images indicate that the corresponding large-scale disturbances in the EUV covered vast areas in the central and northern disk sectors over several tens of minutes. We can see from the 195 Å heliogram (Fig. 3c) that deep dimmings formed in the transequatorial structures between regions 696 and 695, in the neighborhood of these regions, and in some remote areas. As this took place, some loops between regions 696 and 695 remained unaffected by the dimmings, or even increased in brightness after the CME eruption.

In the southward direction, the dimming disturbances reached the point 1 near the northwestern boundary of the coronal hole CH1 (Fig. 1). In the northward direction, a deep dimming first encompassed the area 2, then extended into the large high-latitude zone 2–3–4 between coronal holes CH3 and CH4 in the form of diffuse darkenings. In the eastward direction, a narrow dimming can be traced up to point 5.

The development of dimmings to the west of region 696 was accompanied, mainly in the interval 01:26–02:24 UT, by the emergence and slight, gradual westward displacement of the narrow glowing chain 6–7 located along the eastern boundary of the transequatorial coronal hole CH2. Appreciable brightness decreases are also present over the western/northwestern limb and in the neighborhood of the remote region 693 located to the southwest of CH2.

The pattern of dimmings in all four various-temperature EIT channels can be traced using the heliograms closest to this eruptive event obtained on November 5 at ~19 UT as the background images. In doing so, we should bear in mind that the next set of heliograms refers to November 6, ~01 UT, by which time the development of the dimmings was not yet completed, so that a 6–19-min difference between the observation times in different channels can have a considerable effect on the observed structure and location of the dimmings. The corresponding derotated fixed-difference images are given in the upper row in Fig. 4. We can see from these images that by the time indicated in the heliograms, transequatorial dimming structures coincident in shape and location formed between regions 696 and 695 in all three coronal

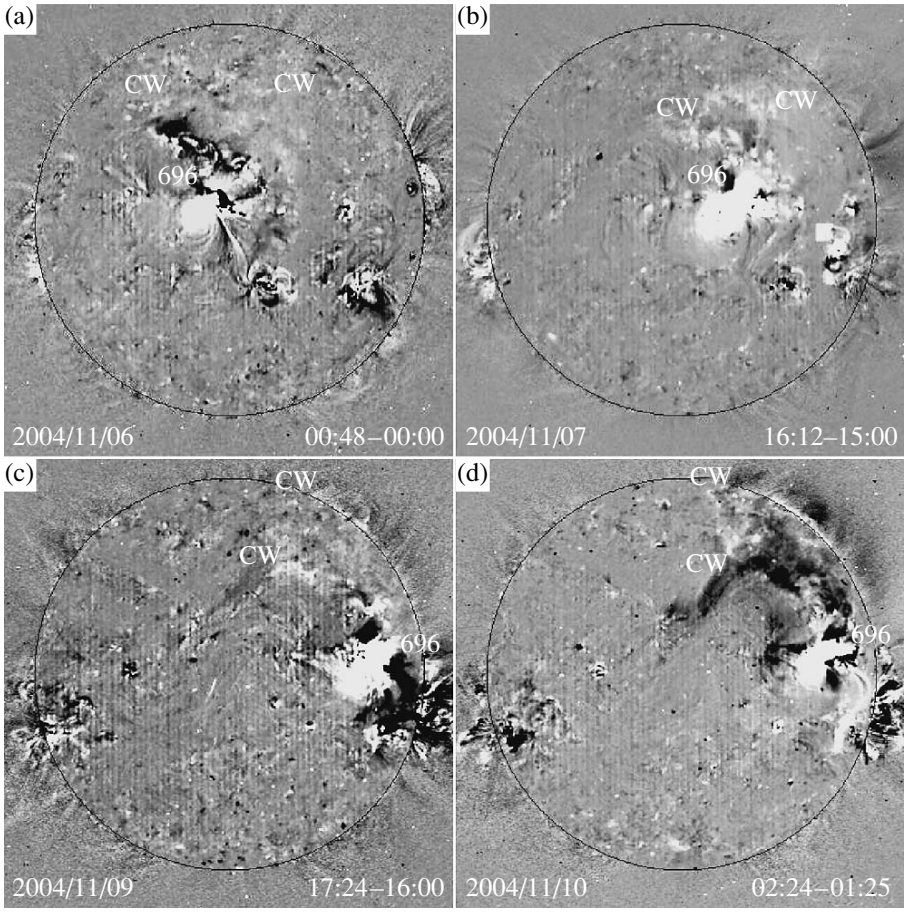

Fig. 5. Derotated fixed-difference SOHO/EIT images in the 195 Å channel showing coronal waves (CW) and dimmings in four eruptive events of November 2004. The time is indicated as in Fig. 2.

channels—171 Å (Fig. 4b), 195 Å (Fig. 4c), and 284 Å (Fig. 4d). In the 284 Å channel, we can also see an analog of the chain 6–7 described above, located, as at 195 Å (Fig. 3c), along the eastern boundary of the transequatorial coronal hole CH2 (Fig. 1). The brightest, southern, fragment of this chain is also present in the 171 and 195 Å channels. Apparently, the system of dark loops to the south/southeast of region 696 (especially in the 171 and 195 Å channels) and the dimmings that stretch eastward from region 696 represent dimmings that are completely or partially coincident in the coronal channels.

In connection with the large-scale disturbances in the northern half of the disk, we note that the bright chain, that is present in the 171 and 195 Å channels (Figs. 4b, 4e) and stretches from region 696 along the northwestern boundary of CH4, seems to be not related to the considered eruptive event. This chain reflects emission variations that occurred between the times of the base images chosen in this case (November 5, ~19 UT) and the beginning of the considered event. This interpretation is supported by the fact that this chain is virtually invisible in the 195 Å difference heliograms (Fig. 3c) obtained at 12-min intervals relative to the base image of November 6 at 00:00 UT.

At the same time, the 6-h difference images in the three coronal channels (Figs. 4b–4d) reveal, though not so clearly, fragments of the northern system of diffuse dimmings. This covers an extensive sector between region 696 and the two coronal holes CH3 and CH4. At this stage, the deep dimmings near and to the north of region 696 can only be seen in the high-temperature 284 Å channel (Fig. 4d). It is noteworthy that in the 304 Å transition-layer channel (Fig. 4a), a pronounced large-scale dimming consisting of several dark structures diverging toward the pole is observed instead of fragmented coronal dimmings, almost everywhere in the northern disk sector 2–3–4. At the same time, the southern transequatorial system of coronal dimmings between regions 696 and 695 is almost invisible in the 304 Å transition-layer channel.

The images (put on the web site only) representing the differences between November 5 at 19 UT and the next session of observations in the various-temperature channels one 6-h interval later show that both main dimming systems (the transequatorial southern and the fragmental northern one) in the three coronal channels—171, 195, and 284 Å—still existed and basically retained their structures and locations at least until 07 UT on November 6. At the same time, the northern dimmings were weakly manifest in the 304 Å transition-layer channel, but a portion of the southern transequatorial dimming structure was visible.

The sequence of 12-min difference heliograms in the 195 Å channel can be used to gain some (very limited) information about the coronal wave. In this event, the corresponding disturbance can be seen in three frames between 00:48 UT and 01:26 UT (Fig. 5a) as a diffuse brightening that propagates from the eruption center toward the northern polar region. It is important that the propagation of the coronal wave was anisotropic, within the same sector between CH3 and CH4, where the transit of the wave was followed by the development of the northern system of fragmented dimmings. According to crude estimates, the propagation speed was several hundred km/s, which is usual for UV coronal waves.

4.2. Event of November 7, 2004

A largely similar pattern of dimmings and a coronal wave was present on November 7 after an X2.0 flare (with its maximum at 16:06 UT; coordinates N09 W17) and a powerful full-halo CME with a bright expanding loop structure over the northwestern limb (Fig. 2d). Derotated difference images in the 195 Å channel indicate that this eruptive event was accompanied by the development of the same two basic large-scale dimming systems that were observed during the preceding event (the southern transequatorial and northern high-latitude systems). By 18:00 UT, these dimmings appeared as is shown in Fig. 3d. Here, the southern dimming system does not occupy the entire space between regions 696 and 695, as was the case in the event of November 6, but consists of two components. One of them (8) has a relatively small area and is located to the south of region 696. The other, more extended, dimming component (1–7) is observed in the region where the bright transient chain was present during the event of November 6. It stretches along the eastern boundary of the transequatorial hole CH2 (Fig. 1), curves around the region 695 on the east, and reaches the southern coronal hole CH1. These two components are connected by one or two narrow dimming channels. In the initial stage of the event, at 16:00–16:12 UT, a bright compact surge propagated between these two dimming components along a curved, S-shaped trajectory from the eruption center in region 696 to the southern region 695.

The northern dimming system in this event was far better developed than in the event of November 6. We can see from Fig. 3d that deep dimmings cover a vast space in the northern half of the disk. This area is bounded by CH3 from the west and by CH4 from the east; in the meridional direction, it extends from the northern polar region to the altitude of active region 696 and the southern boundary of the eastern coronal hole CH4. This dimming system consists of several extended, interrelated, and intersecting structures. Most pronounced is the dimming 9–2–3, which runs from the eruption center to CH4 and then to the northern polar region. Another extended meridional dimming, 10–4, stretches into the same polar region along the eastern boundary of CH3. In the eastern direction, the dimming first reaches the dark core 11 and then outlines the loop structure 11–5. The dimming 9–2–3 probably also partially encompasses the northward directed large-scale loops running from the eruption center to the southern neighborhood of CH4. Various dimming structures related to this event were also observed over a long segment of the western limb, from the neighborhood of region 693 on the south to the northern polar region. On the whole, the range of position angles in which the bright loop structure of the CME was observed (Fig. 2d) corresponds to the sector of the disk where the large-scale dimmings were located.

This dimming pattern can also be identified in the derotated difference heliograms taken at 6-h intervals in the four EIT channels (Fig. 4, lower row). In the three coronal channels—171 Å (Fig. 4f), 195 Å (Fig. 4g), and 284 Å (рис. 4h)—the main dimmings of both the southern and northern systems are largely similar in their shapes and locations. The southern transequatorial dimmings between regions 696 and 695 and the dimming structures over the northwestern sector of the limb are best developed in the high-temperature channels of 195 and 284 Å, while two branches of the northern dimming system are also clearly visible in the moderate-temperature channel of 171 Å. In the highest-temperature channel of 284 Å, a diffuse dimming arc is displayed, which stretches from the eruption center toward the western boundary of the northeastern coronal hole CH4. In the transition-layer channel, 304 Å (Fig. 4e), distinct, although relatively small in area, fragments of the southern and northern dimming systems can be seen; these likely correspond to the deepest portions of the coronal dimmings.

The coronal wave is displayed in the 195 Å channel at 16:12–16:36 UT. Figure 5b shows that, apart from the diffuse brightening, it has a sharp, loop-shaped front. It is noteworthy that, as in the preceding event, this coronal wave can be observed within the limited angular sector that corresponds to the northern dimming system and propagates in the same space between CH3 and CH4. The coronal wave precedes the main dimmings, although some diffuse dimming structures emerge ahead of the coronal-wave front.

4.3. Events of November 9 and 10, 2004

These two very similar significant eruptive events occurred over a very short interval of approximately nine hours. The corresponding flares in region 696 took place on November 9 at ~17 UT (class 2N/M8.9; coordinates N07 W51) and November 10 at ~02 UT (3B/X2.5, N09 W49), and both CMEs can be described as full halos with the most pronounced high-speed eruption over an extended sector of the western limb (Figs. 2e, 2f).

The derotated fixed-base difference heliograms taken in the 195 Å channel demonstrate that the large-scale activity in both these events had nearly the same character as in the preceding events. In the event of November 9 (Fig. 3e), a deep and extensive transequatorial dimming encompassed the entire space between regions 696 and 695 and the corresponding sector over the western limb. The main northern dimmings formed along large-scale loop structures that stretched from the eruption center (region 696) toward the western boundary of CH4 (Fig. 1), which was at that time near the central meridian. These giant loop structures can be clearly seen in the original 195 and 284 Å heliograms of November 9 and 10, which are present on the web site. In particular, the large-scale dimming arc 10–12–5 stands out. The eruption also involved the loops connecting the remote dimming branch 12–5 and the dimming 10–11, which abuts on the eruption center. The development of the dimming branch 12–5 probably continued in the southern half of the disk, to the dimming focus 13. As in the preceding events, fragmented dimmings also involved the northern high-latitude sector, west of CH4, and the corresponding northwestern sector of the limb.

The dimming pattern in the 195 Å channel largely repeated itself in the event of November 10 (Fig. 3f); it was even substantially enhanced in the northern system, although the time interval between these two events was short. In the transequatorial space between regions 696 and 695, the well-defined dimming 1 is visible only near the eruption center, and the glowing transequatorial loops and the bright southern substrate in the fixed-base difference images seem to reflect the continuing recovery of brightness after the dimming that occurred during the preceding eruption, rather than a real brightening of these structures related to this event. On the other hand, all the dimmings constituting the northern system have become much more distinct and deep, i.e., dark. This is true, in particular, for the giant dimming arc 10–12–5, the loop structure 10–12–11, the high-latitude dimming 12–3 at the boundary between CH4, and the dimming over the northwestern sector of the limb. The distant southern dimming focus 13 is again visible in this event; it is probably connected by relatively weak, extended fragmented dimmings with the northern arc-shaped dimming 10–12–5 and the southern dimming 1 adjoining to the eruption center.

Difference heliograms for both events taken at 6-h intervals in the four various-temperature EIT channels, similar to those shown in Fig. 4, are present on the web site. An analysis of these shows that the main dimmings also coincided almost completely in the events of November 9 and 10 as observed in the coronal channels—171, 195, and 284 Å; this is also the case for the fragmented manifestations of these dimmings in the transition-layer channel 304 Å.

Both events were accompanied by coronal waves in the 195 Å channel (Figs. 5c, 5d), which exhibited the same characteristics as in the preceding events. In both cases, an appreciable coronal wave was visible only north of the eruption center, and propagated toward the northern polar sector along the structures that were also involved in the developing dimmings. Figure 5d illustrates the stage of the event of November 10 at which the coronal-wave front reached the western boundary of CH4 and, possibly for this reason, became brighter.

5. DISCUSSION AND CONCLUSION

Based on our analysis, we can summarize the most important characteristics of the large-scale activity in the series of eruptive events of November 2004 as follows.

(1) The major CMEs and the corresponding flares were accompanied by large-scale disturbances that were global in the EUV and encompassed a substantial portion of the solar disk, far exceeding the size of the main active region.

(2) Dimmings were observed in two large-scale systems: (a) the southern transequatorial system connecting the eruption center in the northern half of the disk with a remote active region located on the other side of the heliographic equator and (b) the northern system, which covered a large space

between the eruption center, two coronal holes, and the northern polar region. As is usual [11, 26], the relative brightness reduction in the main dimmings (their depth) was several tens of percent.

(3) In each event, both the southern and northern dimmings were displayed nearly identically in the three coronal channels at 171, 195, 284 Å, which correspond to different line-excitation temperatures. The deepest fragments of these dimmings were also observable in the transition-layer channel at 304 Å.

(4) In the events considered, the coronal waves were anisotropic and propagated from the eruption center in the northward direction only, in the same disk sector between the two coronal holes where the northern dimming system formed.

(5) A number of additional peculiar properties were revealed, such as the formation of a bright, transient, transequatorial chain along the boundary of the equatorial coronal hole in one of the events of November 6, 2004; the presence of a large-scale northern polar dimming in the transition-layer channel during the same event, which considerably exceeded in depth and area the corresponding dimmings in the three coronal channels; and departures/oscillations of the coronal rays far from the eruption center under the action of a CME.

To begin our discussion of these observational results, we note, first of all, that the large scale of the disturbances provides evidence that the eruption of major CMEs involves global structures of the solar magnetosphere that connect, in particular, the eruption center with remote areas of the disk and coronal regions. As this occurs, dimmings affect, first and foremost, these structures, which have enhanced brightness on the background, pre-event heliograms [4, 21]. In the case considered, an ensemble of bright, transequatorial loops corresponds to the southern dimming system; these stretch from the eruption center (region 696) to active region 695. Such an inclusion of transequatorial loops in the CME-eruption process has also been observed in other events. For example, according to [27], the instability of such loops can trigger the eruption of individual CMEs. In the northern dimming system, especially in the events of November 9 and 10, 2004, giant loops connecting the eruption center and the southern neighborhood of CH4 stand out. As in some other events [21, 29], dimming patches at the remote footpoints of these loops can originate almost immediately after the beginning of dimming development at the footpoints of the loops adjoining to the eruption center. Such a development of dimmings is possible if the upper portions of the loops rise (stretch) in the initial stage of the eruptive event, which results in a quasisimultaneous decrease of the emission measure and brightness at both footpoints of these loops.

The observed coincidence of the main dimmings in the three coronal channels sensitive to different-temperature plasmas testifies that the decreases in the brightness of dimming structures are due to decreases in the emission measure rather than temperature variations [12, 14, 26]. In principle, such a decrease could occur as closed magnetic structures expand in the initial stage of the CME. However, this process can only result in relatively short-lived dimmings. The evacuation of material along opened (stretched) field lines in the magnetic structures that constitute the erupting CME is considered the most plausible mechanism for the origin of long-lived dimmings with lifetimes measured in hours. It is for this reason that such dimmings are called transient coronal holes. A direct confirmation of this interpretation of dimmings is the outflow of plasma from them deduced in [30, 31] based on the Doppler shifts of several lines that can be recorded by the SOHO/CDS spectrometer. It also cannot be ruled out that some dimmings are due to the CME-related inhibition of plasma heating and/or material inflow into the corresponding structures [32]. The manifestations of the deepest dimmings observed also in the low-temperature channel of 304 Å indicate that the CME eruption and the dimming-formation processes induced by the eruption affect both the coronal and the transition-layer plasma [12].

Two types of coronal waves can be distinguished based on the currently available studies of coronal waves in the EUV range, in particular, comparing them to dimmings and Moreton waves observed in the chromospheric Hα emission [21]: (a) a wave mode that propagates independently of dimmings and is identified with a MHD disturbance and (b) an eruptive mode that develops at the frontal boundary of expanding dimmings in the process of a sequential opening of magnetic field lines as the CME rises. In the series of events of November 2004 analyzed here, the coronal waves should probably be attributed to the eruptive type, since they propagated along the same northern structures between two coronal holes, CH3 and CH4, where they were followed by the developing northern dimming system. One should make a reservation that this statement cannot be regarded as definite, since EIT observations at 12-min intervals, recording coronal waves in only two or three frames, are usually insufficient for a detailed analysis of these waves. We note that the coronal waves in the eruptive events of November 2000 [18] and October 2003 [3, 4] were probably explosive, and propagated in a disk sector where virtually no dimmings emerged and no active regions were present.

The properties of the events of November 2004 described above suggest that they were homologous. This follows from the similarity of the main large-scale disturbances in the recurrent events of this series. In particular, starting from the events of November 3, 2004 (Figs. 3a, 3b), the shape and location of both the southern and northern dimming systems were similar virtually in all cases, the coronal waves propagated similarly in the northern disk sector only, and an identical appearance was noted for halo CMEs with bright loop structures over the most extensive, northern dimming system. Such large-scale homology seems to be typical of serial eruptive events. In particular, it was among the main characteristics of the events of November 2000 [18] and October and November 2003 [3, 4]. The observed homology implies that conditions for a new eruption of the same coronal structures of the global solar magnetosphere form during the interval between two successive events. The example of the events of November 9 and 10, 2004 indicates that this interval can be very short—about nine hours. In the case of dimmings and coronal waves, the homology indicates that large-scale structures can completely or partially recover their brightness during this interval, and the type of coronal waves and their anisotropic distribution within a restricted angular sector are due to the similar character of the energy release in the CME processes and the preserved properties of the global solar magnetosphere. The specific mechanisms responsible for the homology of large-scale disturbances in repeated eruptive events remain incompletely understood, and require further investigation.

Up to now, the formation of narrow transient chains has mainly been observed during the interaction of large-scale eruptive disturbances with polar coronal holes [14]. In the event of November 6, 2004, such a chain was observed over about an hour at the boundary between the developing southern dimming system and the transequatorial coronal hole CH2. Obviously, this chain formed during the intense interaction between two different magnetic structures—the open field lines of the long-lived coronal hole and the gradually opening magnetic field of the developing dimming. Such an interaction can result, particularly, in the compression of plasma and magnetic reconnection at the boundary of the interacting magnetic fluxes, accompanied by an intense energy release. In all probability, the same process can take place during the formation of eruptive-type coronal waves.

A huge northern dimming was recorded in the event of November 6, 2004 in the transition-layer 304 Å channel, in only one available frame, 30–40 min after the estimated eruption time. This does not provide information about its dynamics. A similar dimming observed in the same channel by the CORONAS-F/SPIRIT telescope during the event of November 18, 2003 [4] had a transient nature, propagated from the eruption center at a speed of about 200 km/s, and, in all probability, was conditioned by the absorption of radiation in the cold plasma of the erupting filament. The dimming of November 6, 2004 may have had a similar nature, and was also related to the absorption of radiation in the tail portion of the detached CME.

The deviation or even "blowing out" of coronal rays under the action of a CME was discovered even from the coronagraph/polarimeter data onboard the orbiting observatory Solar Maximum Mission [28]. Based on the example of the series of events considered here, the higher-quality observations with the SOHO/LASCO high-sensitivity coronagraphs covering much broader ranges of heliocentric distances demonstrate that departures can also be succeeded by oscillations of coronal rays, in particular, at very distant position angles from the central axis of the CME in the plane of the sky. This poorly investigated phenomenon, as well as some other properties of the large-scale activity in the events of November 2004, is worthy of additional targeted studies.

ACKNOWLEDGMENTS

I am grateful to the SOHO/EIT and LASCO teams for making available the data used in the analysis (SOHO is an international cooperative project of ESA and NASA). I am also obliged to V.V. Grechnev (Institute for Solar and Terrestrial Physics, Irkutsk) for the IDL programs used to construct the difference images and for useful discussions of the text of the paper. This work was supported by the Russian Foundation for Basic Research (project no. 03-02-16049), the Ministry of Education and Science of the Russian Federation (grant no. NSh-1445.2003.2), and the basic-research programs of the Russian Academy of Sciences "Nonstationary Phenomena in Astronomy" and "Solar Activity and Physical Processes in the Sun–Earth System."

REFERENCES

1. I. S. Veselovskii, M. I. Panasyuk, S. I. Avdyushin, *et al.*, Kosm. Issled. **35**, 453 (2004) [Cosmic Res. **42**, 435 (2004)].
2. Yu. I. Yermolaev, L. M. Zelenyi, G. N. Zastenker, *et al.*, Geomagn. Aeron. **45**, 20 (2005).
3. I. M. Chertok and V. V. Grechnev, Astron. Zh. **82**, 180 (2005) [Astron. Rep. **49**, 155 (2005)].
4. V. V. Grechnev, I. M. Chertok, V. A. Slemzin, *et al.*, J. Geophys. Res. **110**, A09S07, doi:10.1029/2004JA010931 (2005).
5. J.-P. Delaboudinière, G. E. Artzner, J. Brunaud, *et al.*, Sol. Phys. **162**, 291 (1995).

6. I. A. Zhitnik, O. I. Bougaenko, J.-P. Delaboudiniere, *et al.*, in *Proceedings of the 10th European Solar Physics Meeting, Prague, Czech Republic, 2002* (ESA Publ. Divis., Noordwijk, 2002); ESA SP-506, Vol. 2, p. 915 (2002).
7. D. F. Webb, J. Atmos. Sol.-Terr. Phys. **62**, 1415 (2000).
8. A. S. Sterling, J. Atmos. Sol.-Terr. Phys. **62**, 1427 (2000).
9. N. Gopalswamy and B. J. Thompson, J. Atmos. Sol.-Terr. Phys. **62**, 1458 (2000).
10. H. S. Hudson and E. W. Cliver, J. Geophys. Res. **106**, 25199 (2001).
11. I. M. Chertok and V. V. Grechnev, Astron. Zh. **80**, 162 (2003) [Astron. Rep. **47**, 139 (2003)].
12. I. M. Chertok and V. V. Grechnev, Astron. Zh. **80**, 1013 (2003) [Astron. Rep. **47**, 934 (2003)].
13. N. Gopalswamy, *The Sun and the Heliosphere as an Integrated System*, Ed. by G. Poletto and S. Suess (Kluwer, Dordrecht, 2004); ASSL Ser. (2004), p. 201.
14. B. J. Thompson, S. P. Plunkett, J. B. Gurman, *et al.*, Geophys. Res. Lett. **25**, 2465 (1998).
15. A. Klassen, H. Aurass, G. Mann, *et al.*, Astron. Astrophys. **141**, 357 (2000).
16. A. Warmuth, B. Vršnak, J. Magdalenić, *et al.*, Astron. Astrophys. **418**, 1117 (2004).
17. D. A. Biesecker, D. C. Myers, B. J. Thompson, *et al.*, Astrophys. J. **569**, 1009 (2002).
18. I. M. Chertok, V. V. Grechnev, H. S. Hudson, and N. V. Nitta, J. Geophys. Res. **109**, A02112, doi:10.1029/2003JA010182 (2004).
19. G. E. Moreton and H. E. Ramsey, Publ. Astron. Soc. Pac. **72**, 357 (1960).
20. C. Delannée, Astrophys. J. **545**, 512 (2001).
21. A. N. Zhukov and F. Auchère, Astron. Astrophys. **427**, 705 (2004).
22. P. F. Chen, C. Fang, and K. Shibata, Astrophys. J. **622**, 1202 (2005).
23. G. E. Brueckner, R. A. Howard, M. J. Koomen, *et al.*, Sol. Phys. **162**, 357 (1995).
24. Yu. I. Yermolaev, L. M. Zelenyĭ, G. N. Zastenker, *et al.*, Geomagn. Aeron. (2005) (in press).
25. I. M. Chertok and V. V. Grechnev, Sol. Phys. **229**, 95 (2005).
26. D. M. Zarro, A. C. Sterling, B. J. Thompson, *et al.*, Astrophys. J. **520**, L139 (1999).
27. J. I. Khan and H. S. Hudson, Geophys. Res. Lett. **27**, 1083 (2000).
28. A. J. Hundhausen, *The Many Faces of the Sun*, Ed. by K. Strong *et al.* (Springer-Verlag, New York, 1999), p. 143.
29. T. Wang, Y. Yan, J. Wang, *et al.*, Astrophys. J. **572**, 580 (2002).
30. L. K. Harra and A. C. Sterling, Astrophys. J. **561**, L215 (2001).
31. R. A. Harrison, P. Bryans, G. M. Simnett, and M. Lyons, Astron. Astrophys. **400**, 1071 (2003).
32. A. M. Uralov, V. V. Grechnev, and H. S. Hudson, J. Geophys. Res. **110**, A05104, doi:10.1029/2004JA010951 (2005).

Translated by A. Getling